IJNRD.ORG ISSN : 2456-4184
INTERNATIONAL JOURNAL OF NOVEL RESEARCH AND DEVELOPMENT (IJNRD) | IJNRD.ORG
An International Open Access, Peer-reviewed, Refereed Journal

Hafnium (Hf) doped $BaTiO_3$: A study of structural and electrical properties for device application feasibility

Arpita Patel[1#] and Rajesh Kumar Katare[1]

[1]*Department of Physics, SAGE University, Indore, 452001, India*

arpitapatel521@gmail.com

Abstract

Owing to its excellent dielectric and ferroelectric properties, $BaTiO_3$ is one of the most extensively studied ferroelectric materials and is currently utilized in a wide variety of fields including multilayer capacitors, transducers, actuators, electro-optical devices, electromechanical devices, dynamic random-access memory, field-effect transistors, and thermistors, among others. Taking into the consideration these applications, Hf has been selected as the substituent for $BaTiO_3$ ($BaTi_{0.9}Hf_{0.1}O_3$) to modify its physical properties. Hereby, we report synthesis of $BaTi_{0.9}Hf_{0.1}O_3$ using solid state route and investigated its crystallization via XRD and also emphasized on its dielectric and impedance characteristics. XRD analysis reveals tetragonal crystal structure of the synthesized sample. Dielectric measurements as a function of frequency infer the sample to inherit higher dielectric permittivity with relatively. Conduction mechanism was investigated using electric modulus and impedance studies. Impedance study reveals non-ideal Debye-like behavior of the ceramic.

Keywords: Synthesis; ferroelectrics; dielectric properties; crystal structure; Impedance

Introduction and review

Barium titanate ($BaTiO_3$) ceramics have been extensively used as important ferroelectric materials for decades, which is used as capacitor, ferroelectric memory and so on, because of their excellent dielectric, piezoelectric and ferroelectric properties. The microstructures, dielectric properties of barium titanate can be modified by a wide variety of substitutions possible at Ba^{2+} on A-sites or Ti^{4+} on B-site independently or simultaneously in perovskite structure. Effect of the doping of Sr^{2+}, Pb^{2+}, Ca^{2+} for Ba^{2+} and Zr^{4+}, Hf^{4+} for Ti^{4+}, on dielectric properties have been investigated and are often employed to shift the Curie temperature for particular applications[1-4].

In recent years, many studies are focused on preparation, microstructures and dielectric properties of $BaZr_xTi_{1-x}O_3$ (BZT) materials. As a result, BZT has high dielectric constant, low dielectric loss and large tunability. Moreover, it is known that the characteristics of the ferroelectric phase transition of BZT ceramics strongly depends on Zr content [5,6]. Hafnium is under zirconium in the periodic table of elements and then the activity of hafnium is weaker than those of zirconium. This maybe lead to enhance the covalent bond of B–O, therefore, the properties of barium hafnate titanate ($BaHf_xTi_{1-x}O_3$) possibly are better than that of barium zirconium titanate. Therefore, the structures and electric properties of BHT ceramics have to be investigated in detail. However, the dielectric and ferroelectric properties of BHT ceramics have not been reported systematically [7-9].

It is noted that more polarization states in invariant critical point can induce a large electrocaloric response in ferroelectric ceramics under the relatively low electric field, such as BaH_fTiO_3[10]and $BaSnTiO_3$[11]. In (1-*x*) $BaZr_{0.2}Ti_{0.8}O_{3-x}Ba_{0.7}Ca_{0.3}TiO_3$[12]ceramics system, the excellent. piezoelectric and EC properties can be found around the multi-phase boundary. Similarly, (1-*x*) $BaHf_{0.2}Ti_{0.8}O_{3-x}Ba_{0.7}Ca_{0.3}TiO_3$[13] also shows excellent EC performance near ferroelectric-to-paraelectric phase transition.

Ferroelectrics are promising candidate materials for electrocaloric refrigeration. Materials with a large electrocaloric effect (ECE) near room temperature and a broad working temperature range are getting closer to practical applications[14, 15]. However, the enhanced ECE is always achieved under high electric field, which limits their wide cooling applications[14-16].

Li et. al.[10]has reported$BaHf_xTi_{1-x}O_3$ (*x* = 0, 0.03, 0.06, 0.09, 0.10, 0.11, 0.12, 0.13, 0.15, 0.17, 0.20) samples synthesized by solid state reaction method. They have used precursors as oxides of the materials in the stoichiometric ratios. The synthesized samples have been calcined at 1350 ºC and 1425 ºC with intermediate grinding. The final powder has been transformed into the pellets using polyvinyl alcohol (PVA)as binder. The pellets have been sintered at 1495 ºC for 4h. The final samples have been polished with silver paste to form smooth electric contacts for electrical measurements.

The solid state synthesis of Hf doped $BaTiO_3$materials have been reported by other scientists. Structural studies have shown pseudo cubic nature of the materials. Pristine $BaTiO_3$ is tetragonal in nature. BHT ceramics with *x* = 0, 0.03, 0.11, and 0.17 show pure pseudocubic phase while the BHT ceramics with *x* = 0.03 exhibits the

coexistence of the orthorhombic and tetragonal phases, ant the BHT samples with x = 0.11 and x = 0.17 show a rhombohedral phase at room temperature[7].The XRD Pattern is shown as Figure1

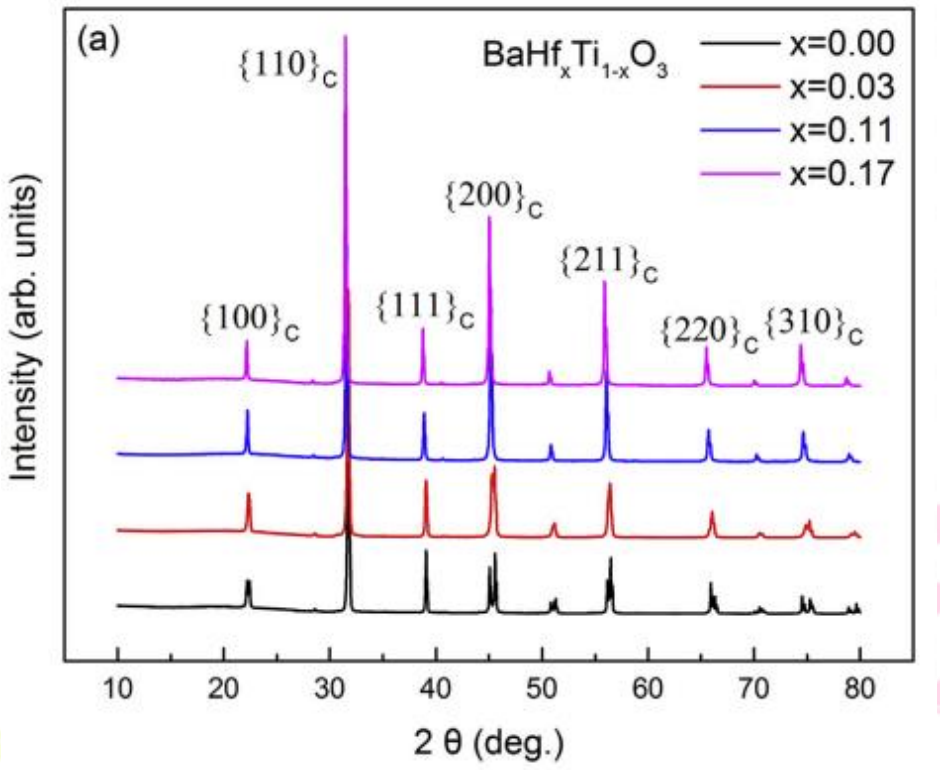

Figure 1: XRD spectrum of$BaHf_xTi_{1-x}O_3$ ceramics [7]

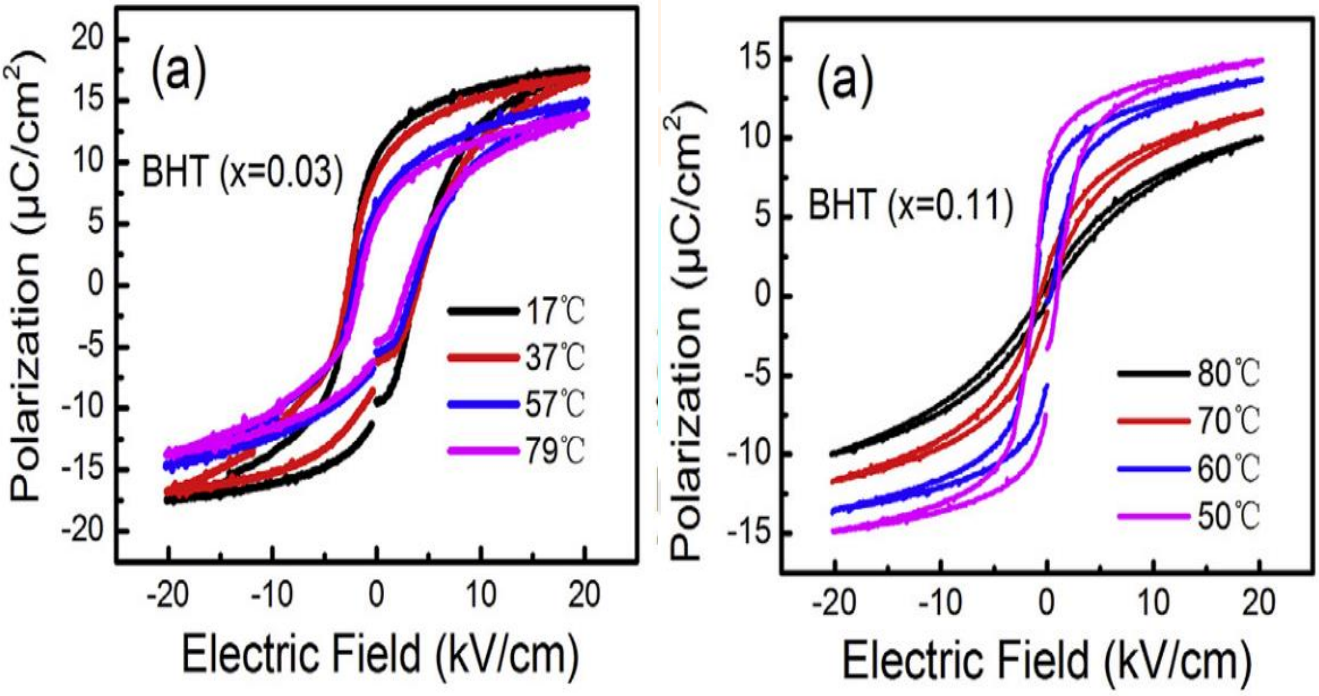

Figure 2: Polarization (P-E hysteresis loop) at various temperatures [10]

In addition to this, the BHT samples with x= 0.03 and 0.11 have been subjected to Polarization (P-E hysteresis loop) studies at different temperatures. The P-E Hysteresis loop of these BHT samples at varied temperatures has been displayed as Figure 2

It is evident from the P-E loop measurements that BHT sample with x = 0.03 inherit more polarization character than BHT sample with x = 0.11. However it is evident that BHT sample with x = 0.03 have higher hysteresis loop due to the possession of large area loop. Furthermore, there seems a transition to more sophisticated soft ferroelectrics with larger Hf concentrations [10].

Wang et. al. [8] also reported Hf based $BaTiO_3$ materials viz. $Ba_{0.85}Ca_{0.15}Ti_{1-x}Hf_xO_3$ synthesized by solid state rote. In the room temperature XRD patterns of $Ba_{0.85}Ca_{0.15}Ti_{1-x}Hf_xO_3$ solid solution, the splitting of the (200) and (310) peaks reveals the existence of tetragonal and monoclinic phase in the BCTH006 ceramics. The overlapping of the diffraction peak around 45^o at x > 0.10 indicates that the structure transforms from tetragonal phase to pseudo cubic one. The XRD pattern is shown as Figure 3.

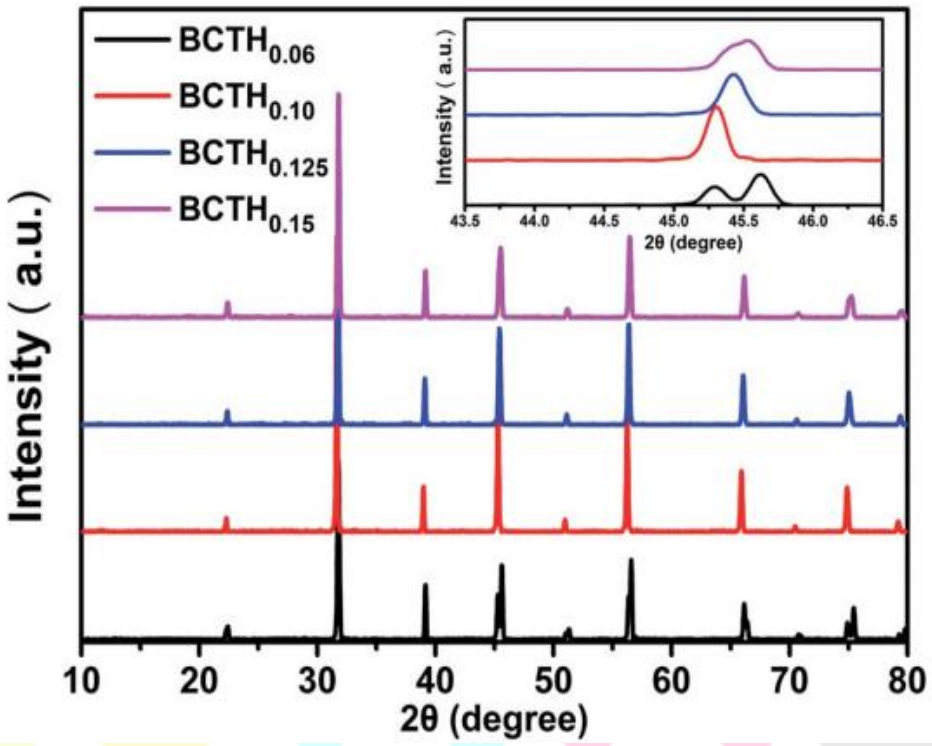

Figure 3: XRD spectrum of $Ba_{0.85}Ca_{0.15}Ti_{1-x}Hf_xO_3$ ceramics [13]

The temperature dependent dielectric studies were reported which reveals the higher dielectric permittivity values. The temperature dependent dielectric permittivity of these samples has been revealed as Figure 4. In this study, the dielectric permittivity was recorded at field values of 10 Hz, 100 Hz, 1000 Hz, 10 000 Hz and 100 000 Hz and 1 V during cooling process. The plots further reveal that with increasing of Hf contents, the Curie temperature decreases gradually. In the dielectric permittivity of BCTH0.15 ceramic, the obvious frequency dispersion is indicates more diffusion of phase transition [8].

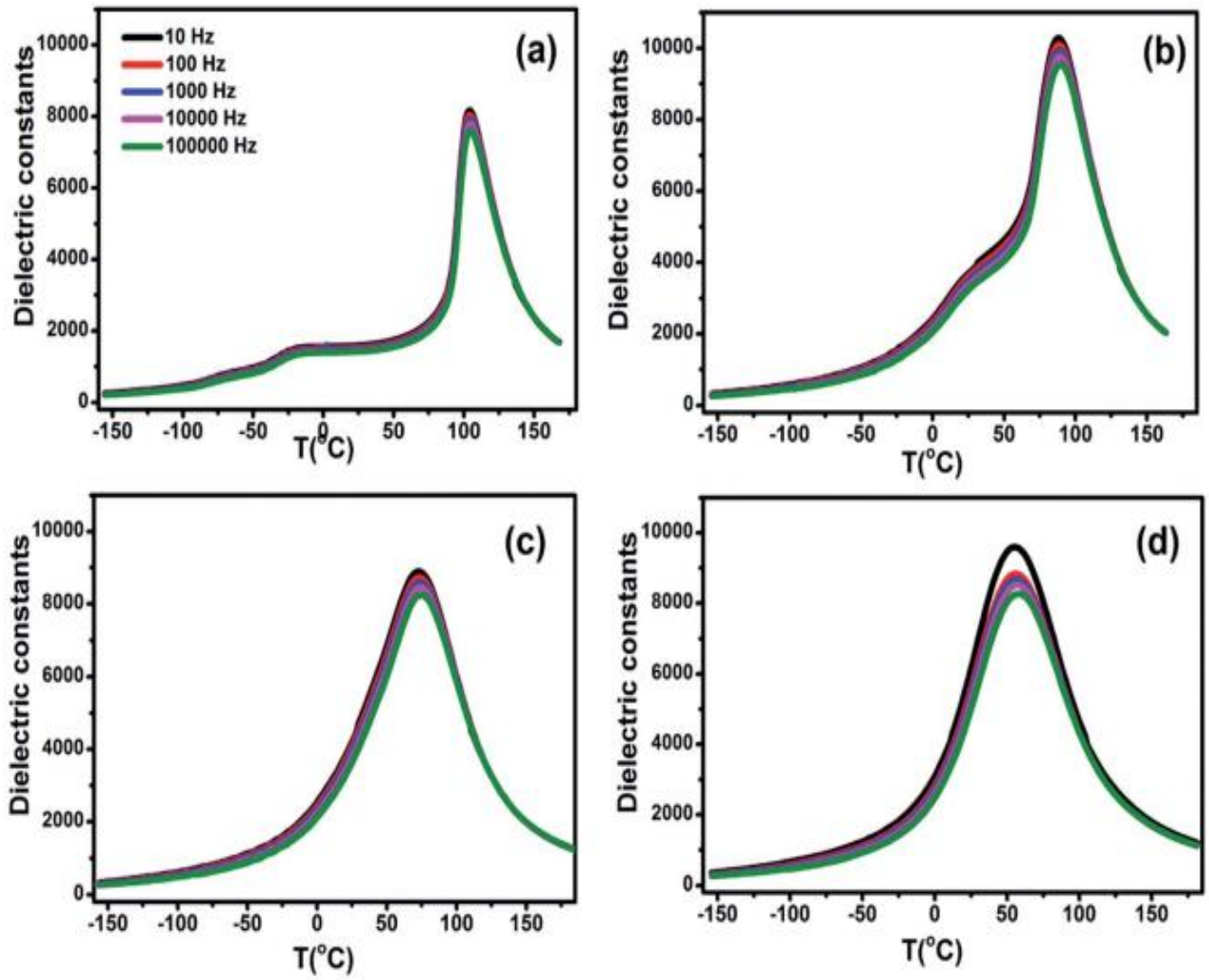

Figure 4: Temperature dependent dielectric permittivity of $Ba_{0.85}Ca_{0.15}Ti_{1-x}Hf_xO_3$ ceramics [8]

Sati et. al. [17] has reported $BaHf_xTi_{1-x}O_3$ ceramics, with x=0.06, 0.12, 0.15, 0.18, 0.21, 0.27 and 0.30. These materials have been synthesized by solid state route. The structural studies of these samples reveal tetragonal structure. Furthermore variation of dielectric constant, dielectric loss, energy bandgap, Urbach energy [The band boundaries semiconductor can have energy disorder, which can be measured using the Urbach Energy. The absorption coefficient as a function of energy is fitted to an exponential function in order to evaluate it. It is frequently employed to explain electron transport in semiconductors with structural disorder] has been studied. The results are displayed as Figure 5.

It is evident from the Figure 5that dielectric constant decreases with increase in Hf concentrations due to the introduction of defects via addition of impurities in the pristine $BaTiO_3$. Same trend as usual if followed by the loss tangent values. The band control over dielectric permittivity is evident. It is observed as the band gap enhances the dielectric permittivity value decline gradually. The trend of the incline is followed by Urbach's energy as Hf content increases.

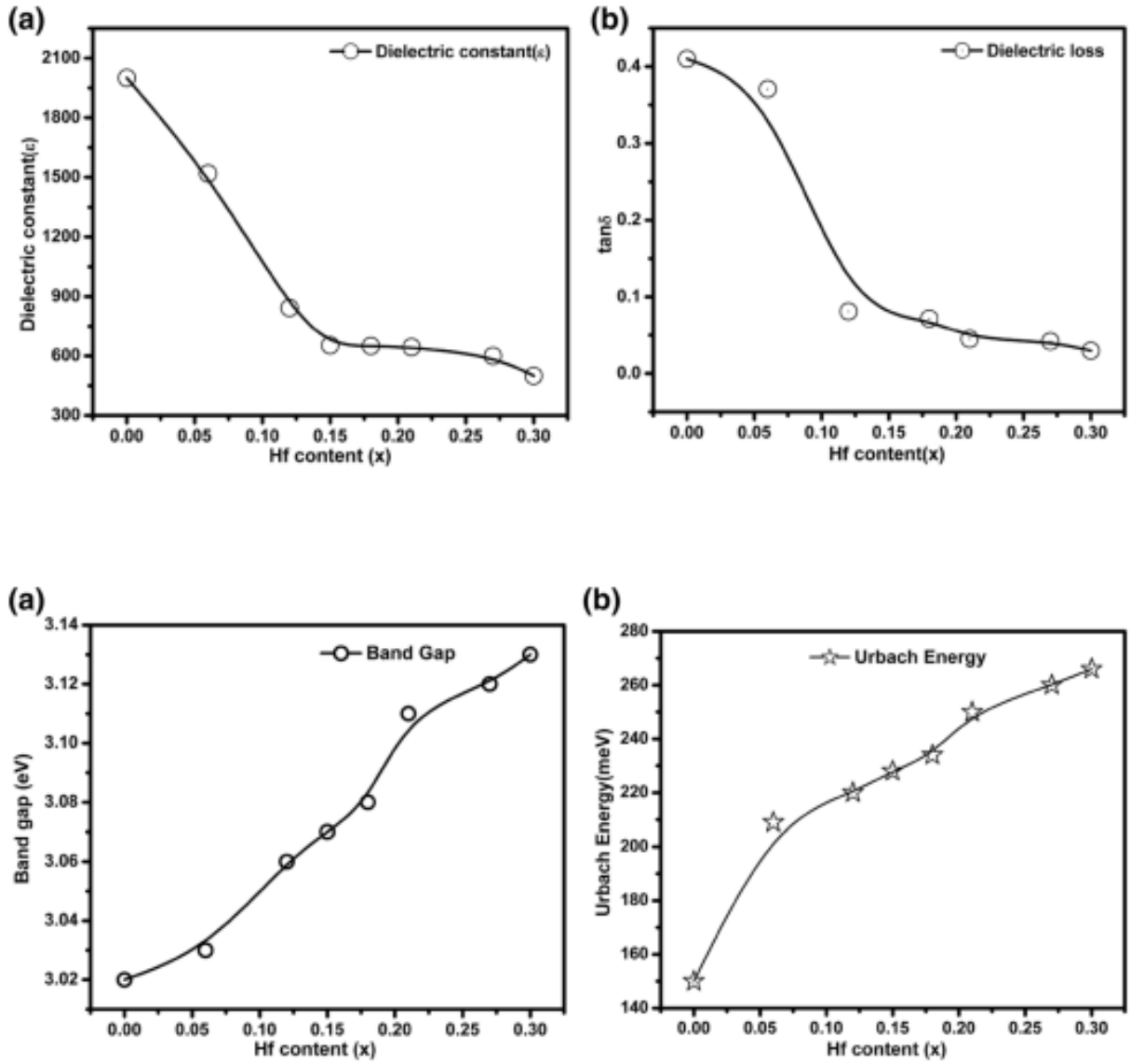

Figure 5: The dielectric constant, dielectric loss, bandgap and Urbach's energy of $BaHf_xTi_{1-x}O_3$ ceramics [17]

Preparation of $BaTi_{0.9}Hf_{0.1}O_3$ ceramic

Hafnium (Hf) doped $BaTiO_3$ synthesized by solid state reaction route. Depicted as

Weighing ⇨ Mixing ⇨ Calcination ⇨ Grinding ⇨ Pelletization ⇨ Sintering

The $BaHf_xTi_{1-x}O_3$ sample material is synthesized using a solid state method in the current investigation. In this instance, amounts specified by the formula were combined in an agate mortar by means of a rigorous five-hour mechanical grinding process. The combined materials were heated at 1100 ^oC for four hours. To create the final fine powder, the powdered combination was ground for duration of thirty minutes. To make pellets, the powder is combined with PVA, a binder. At a pressure of 4-5 tons per inch, round discs with a diameter of 10 mm and a width of 1 mm were created. The resulting pellets were sintered for six hours at 1200 ^oC to produce a hard, compact form of material for use in upcoming experiments.

Structural Analysis of $BaTi_{0.9}Hf_{0.1}O_3$

We have synthesized Hf doped $BaTiO_3$ ($BaTi_{0.9}Hf_{0.1}O_3$) and emphasized on its structural, and electrical properties. The sample has been synthesized by solid state route via double calcination technique.The X-ray data Diffraction spectrum was recorded in the angular range of 10^o-90^o and plotted data has been plotted as Figure 6.The analysis shows tetragonal phase along withthe impurity of $BaCO_3$.The Particle size calculated is 87nm estimated using classical Scherer formula.

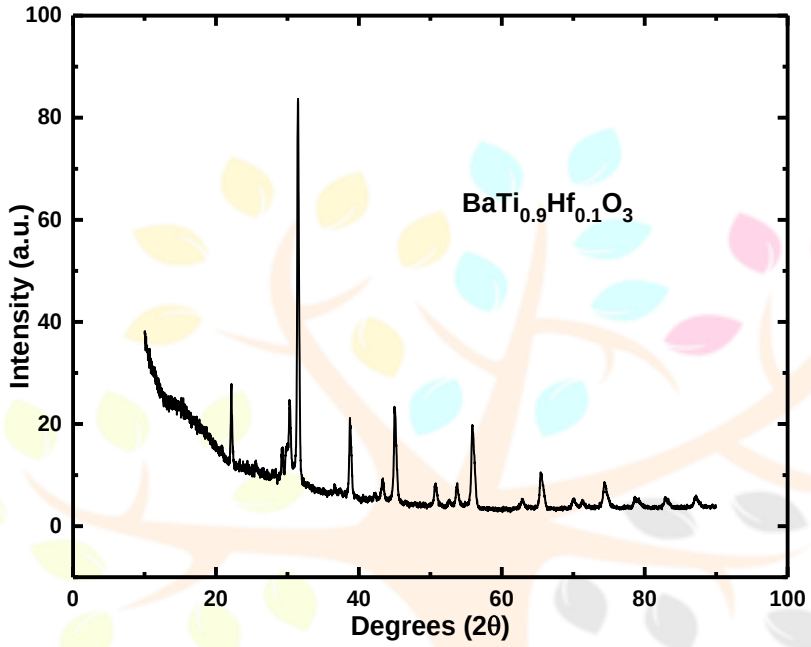

Figure 6: XRD pattern of $BaTi_{0.9}Hf_{0.1}O_3$

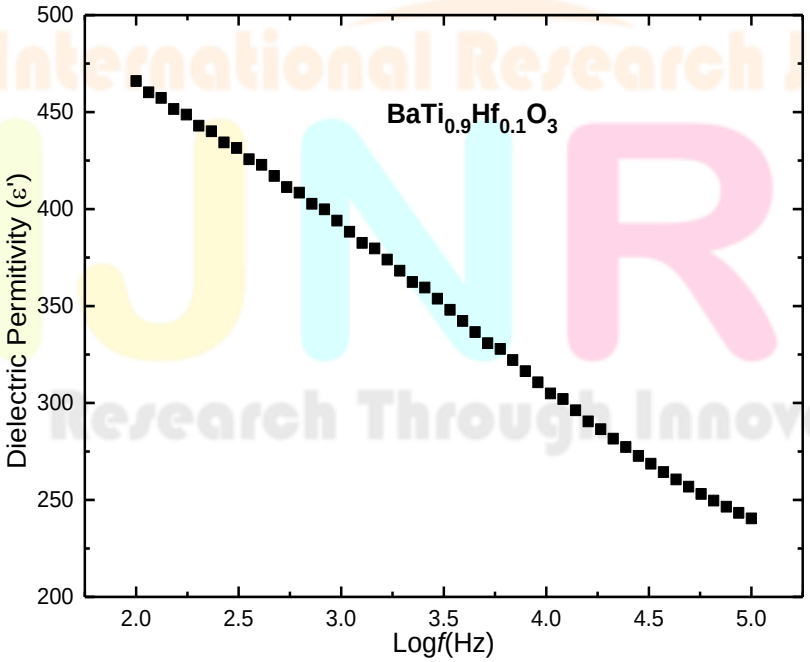

Figure 7: Dielectric permittivity of Hf doped $BaTiO_3$

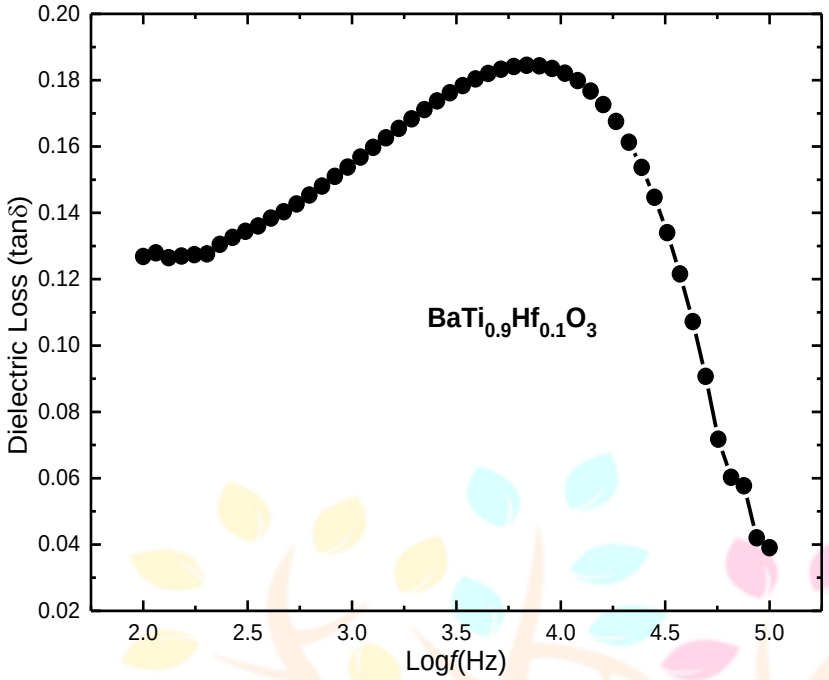

Figure 8: Dielectric loss tangent of Hf doped $BaTiO_3$

Dielectric Studies

The polycrystalline sample $BaTi_{0.9}Hf_{0.1}O_3$ has been investigated for dielectric permittivity studies in the frequency range of 100Hz-10^5Hz. The dielectric permittivity shows a usual trend of decrease with increase in field values. The higher value of dielectric permittivity at low field values is attributed to space charge polarization. The higher value at low frequency and low dielectric permittivity at higher frequency is explained in terms of Maxwell-Wagner Model [18]. According to this model, the free moving charges inside the conducting grains are obstructed by the insulating grain boundaries and results in piling of charge at grain boundaries. At higher values of applied field, the motion of charges is reversed thereby dielectric permittivity decreases as field rises. Actually, polarization comes into existence when charges pile at grain insulating boundaries. Higher the piling, greater isthe polarization that diminishes with increase in the field value [18-20].

Figure 8 shows the fluctuation of tanδ with log*f*. The dielectric loss is extremely high and is observed to rise until it reaches a maximum value, after which it reduces as the frequency of applied field drops. The Koop phenomenological model is consistent with the reduction in the dielectric loss tangent with increasing frequency. Impurities and structural inhomogeneities induce the dielectric loss, which occurs if the polarization lags behind the applied alternating field. At low frequencies, the dielectric loss tangent has a very large value, whereas at higher frequencies, it has a modest loss. At a specific frequency, the dielectric loss in each sample achieves its maximum value. The resonance between the polaron hopping frequency and the applied electric field is responsible for this property[20-22].

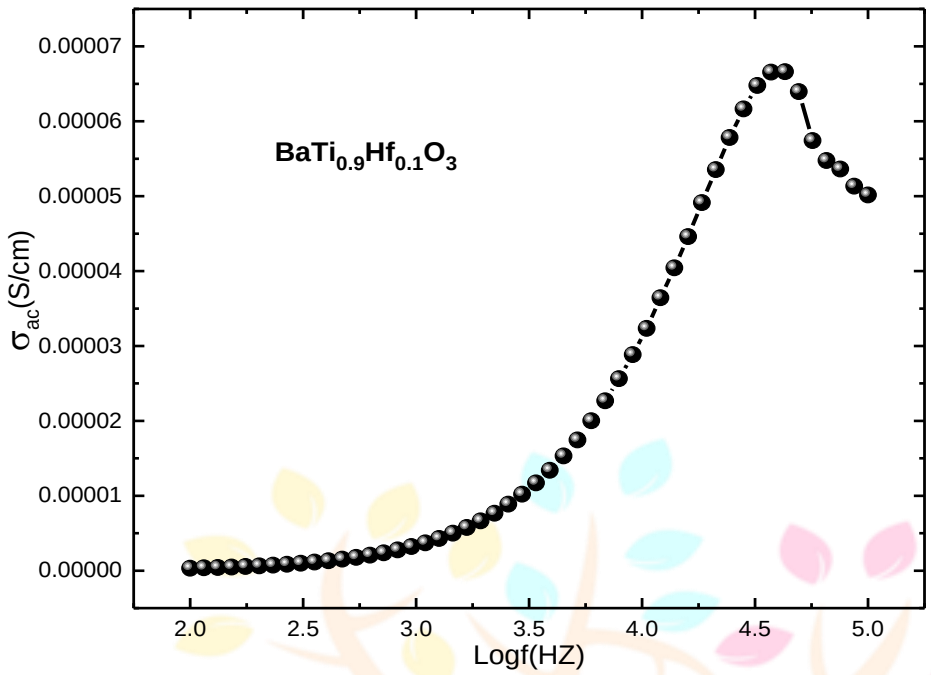

Figure 9: *ac* conductivity of $BaTi_{0.9}Hf_{0.1}O_3$sample

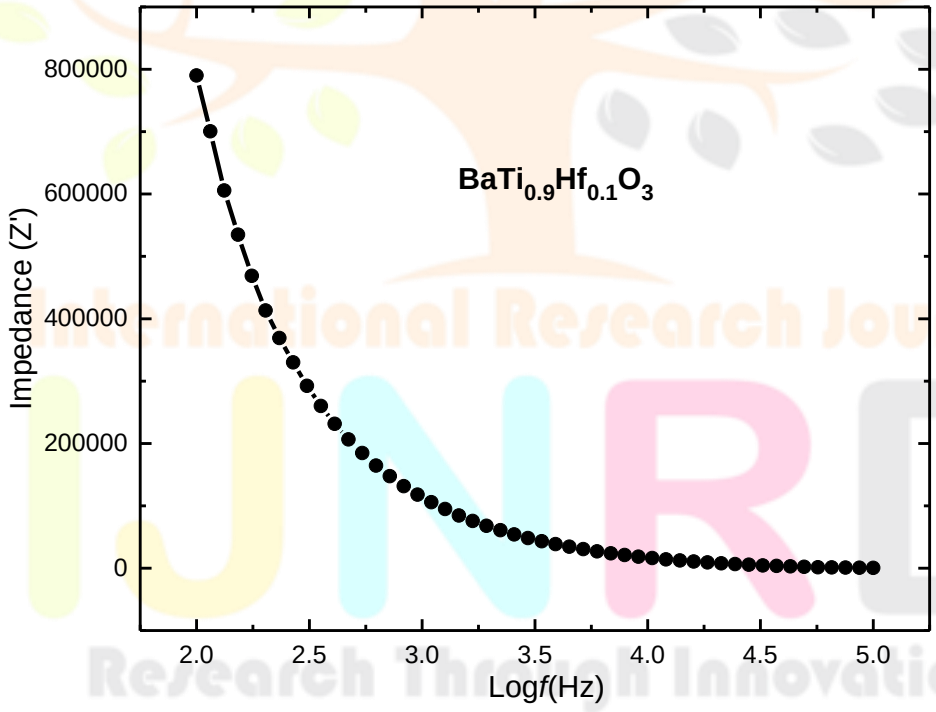

Figure 10: Frequency dependent impedance (real z′) of Hf doped $BaTiO_3$

The *ac* conductivity of the sample as a function of Logf (Hz) has been examined. As shown in Figure 9, the ac conductivity of the sample is initially unaffected by the applied field. However, after the applied frequency

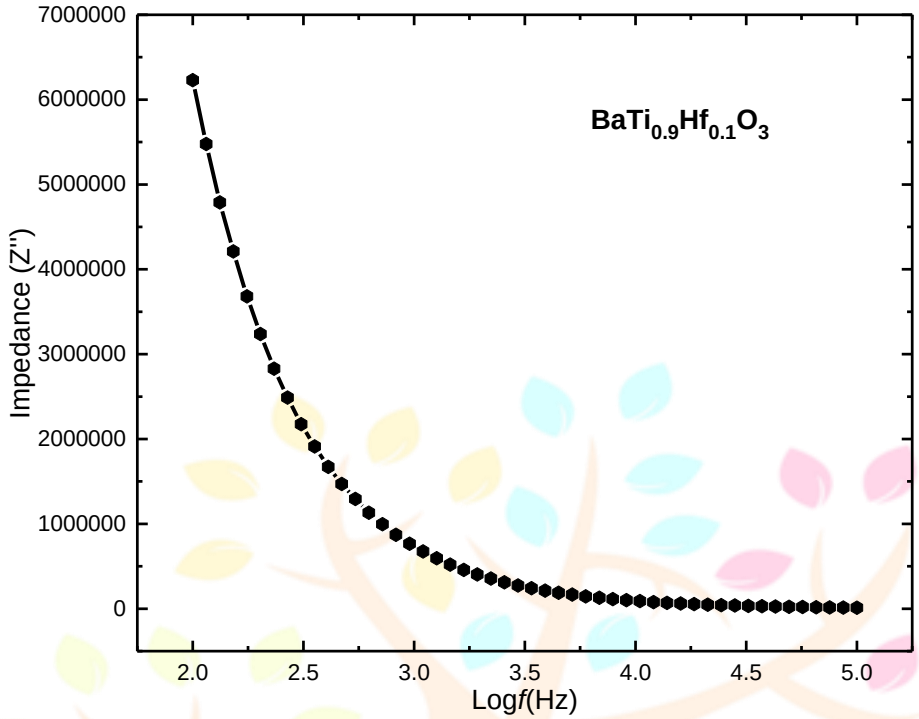

reaches a critical value, thereby trapped charges by the defects and trap centers begin to de-trap and the current then increases quickly as the applied field increases. Furthermore, beyond a certain limit, defects are produced in the system, resulting in the creation of grain boundary defects which hinder the flow of charge carriers reducing the conductivity that is clearly seen visible in the higher field region [20].

Figure 11: Frequency dependent impedance (Imaginary $\tilde{z}$) of Hf doped $BaTiO_3$

Impedance Studies

The complex impedance spectroscopy (CIS) is a vital technique which sheds light on the electrical behaviors of the material. The real and imaginary component of impedance distinguishes the true picture of the sample's physical properties. This technique analyses AC response of a system to a sinusoidal perturbation and further impedance is calculated as a function of perturbation frequency. The variation of real component of impedance (Z') with the frequency is seen in Figure 10. It is seen with rise in temperature the Z' rises and falls which depicts typical negative and positive temperature coefficient behavior (NTCR, PTCR) and AC conductivity rises[20,23].

The real part of impedance monotically decreases with a rise in frequency (>10 kHz) and a constant value is observed (i.e., frequency independent). The trend of merging at higher frequency irrespective of temperature may be due to constant lowering of barrier properties or release of space charge [23-25].

Figure 11 presents the frequency dependent imaginary component of impedance (Z''). The Z'' variation shows represent the distribution of relaxation time. The electrons/immobile charges are dominant relaxation

species at low temperature,whereas at high temperature; this may be the oxygen vacancies or presence of defects. The electrical conductivity may arise due to the hopping of oxygen ion vacancies in localized site [24,25].

In a wide frequency range, the complex impedance spectra (Z″ vs. Z′) were measured and the obtained results are shown in Figure 12. It is evident that the impedance spectrum is characterized by the presence of only one semicircle arc at low frequency values. This kind of impedance response indicates that the grain boundary has a dominant effect on the conduction mechanism, which is probably due to the porous nature of the prepared sample, which was confirmed by structural analysis.

In addition, semicircle centers lie below the real axis of the impedance, and the origin of this depressed semicircle in the complex plane can be attributed to the presence of porosity and inhomogeneities in the samples. The obvious small radius of the semicircle arc is a typical characteristic of most semiconducting oxides. The observed behaviour is non-ideal Debye-like behavior of the ceramics [24-27].

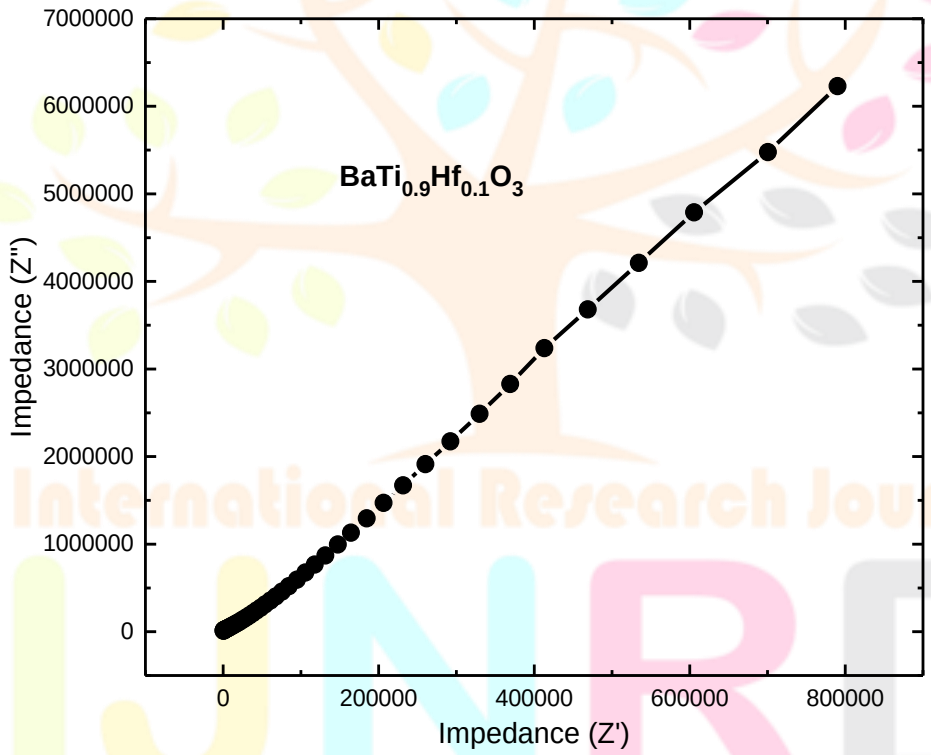

Figure 12: Nyquist's plot of Hf doped $BaTiO_3$

Conclusion

The literature survey of Hf doped $BaTiO_3$ ceramic material with structural, dielectric and optical properties has been carried out and the supporting results are cited in this manuscript. With the motivational results, the successfully solid state route synthesized $BaTi_{0.9}Hf_{0.1}O_3$has been discussed in terms of structural and electrical studies. The single phased $BaTi_{0.9}Hf_{0.1}O_3$sample has been found to crystallize into tetragonal structure(P4mm).The dielectric permittivity has bee witnessed to be relatively high with los tangent values to be comparatively small. Conductivity studies have inferred the sample to be mostly insulating in nature. Impedance

studies carried have been exploited successfully to emphasize on the conduction mechanism in the sample. The sample has been found to be good dielectric material feasible for electronic device applications.

References

[1] W.S. Jung, J.H. Kim, H.T. Kim, et al., Mater. Lett. 64 (2) (2010) 170–172.

[2] S. Anwar, P.R. Sagdeo, N.P. Lalla, Solid. State. Sci. 9 (11) (2007) 1054–1060.

[3] H.T. Jiang, J.W. Zhai, M.W. Zhang, et al., J. Mater. Sci. 47 (6) (2012) 2617–2623

[4] P.R. Ren, H.Q. Fan, X. Wang, et al., Int. J. Appl. Ceram. Technol. 9 (2) (2012) 358– 36

[5] K.H. Chen, T.C. Chang, G.C. Chang, et al., Appl. Phys. A-Mater. 99 (1) (2010) 291–295.

[6] H. Chen, C. Yang, C. Fu, et al., J. Mater. Sci-Mater. El. 19 (4) (2008) 379–382.

[7] J. Chen, C. Fu, W. Cai, G. Chen, S. Ran, Journal of Alloys and Compounds 544 (2012) 82–86

[8] X. Wang, J. Wu, B. Dkhil, C. Zhao, T. Li, W. Lia and X. Lou, RSC Adv., 7 (2017) 5813

[9] P. Mishra and P. Sonia Kumar, J. Alloys Compd., 545 (2012) 210–215.

[10] J. Li, D. Zhang, S. Qin, T. Li, M. Wu, D. Wang, Y. Bai, X. Lou, , Acta Materialia, 115 42 (2016) 58-67.

[11] Z. Luo, D. Zhang, Y. Liu, D. Zhou, Y. Yao, C. Liu, B. Dkhil, X. Ren and X. Lou, Appl. Phys. Lett., 105(10) (2014) 102904.

[12] G. Singh, I. Bhaumik, S. Ganesamoorthy, R. Bhatt, A. Karnal, V. Tiwari and P. Gupta, Appl. Phys. Lett., 102(8) (2013)082902.

[13] P. Wu, X. Lou, J. Li, T. Li, H. Gao, M. Wu, S. Wang, X. Wang, J. Bian, X. Hao, journal of Alloys and Compounds, 725 (2017) 275-282

[14] S.-G. Lu, Q. Zhang, Electrocaloric Materials for Solid-State Refrigeration, Advanced Materials, 21 (2009) 1983-1987.

[15] J.F. Scott, Electrocaloric Materials, Annual Review of Materials Research, 41 (2011) 229-240.

[16] X. Moya, S. Kar-Narayan, N.D. Mathur, Caloric materials near ferroic phase transitions, Nature 6 materials, 13 (2014) 439-450.

[17] A. Sati, A. Kumar, V. Mishra. K. Warshi, A. Sagdeo, S. Anwar, R. Kumar, P. R. Sagdeo, Journal of Materials Science: Materials in Electronics 30(2019)8064–8070

[18] Wagner, K.W.: Ann. Phys. 40, 817 (1913)

[19] Koops, C.G.: Phys. Rev. 83, 121 (1951)

[20] Saleem, M., Mishra, A. and Varshney, D. J. Supercond Nov. Magn. 31, 943 (2018)

[21] Bergman, R.: J. Appl. Phys. 88, 1356 (2000)

[22] Psarras, G.C., Manolakaki, E., Tsangaris, G.M.: Composites A. 34, 1187 (2003)

[23] R. Ranjan, R. Kumar and N. Kumar, J. Alloys Compd. 509 (2011).

[24] M. S. Cao, Z. L. Hou and J. Yuan, J. Appl. Phys. 105, 106102 (2009).

[25] M. S. Cao, W. L. Song and Z. L. Hou, Carbon 48, 788 (2010).

[26] P. B. Macedo, C. T. Moynihan and R. Bose, Phys. Chem. Glasses 13, 171 (1972).

[27] Y. Wei and S. Sridhar, J. Chem. Phys. 99, 3119 (1993).